J. Fluid Mech. (2000), *vol.* 422, *pp.* 125–139. Printed in the United Kingdom

The exact solution of the Riemann problem with non-zero tangential velocities in relativistic hydrodynamics

By JOSÉ A. PONS[1], JOSÉ Mª MARTÍ[1] AND EWALD MÜLLER[2]

[1]Departament d'Astronomia i Astrofísica, Universitat de València, 46100 Burjassot, Spain

[2]Max-Planck-Institut für Astrophysik, Karl-Schwarzschild-Str. 1, 85748 Garching, Germany

(Received 9 August 1999 and in revised form 16 March 2000)

We have generalized the *exact* solution of the Riemann problem in special relativistic hydrodynamics (Martí & Müller 1994) for arbitrary tangential flow velocities. The solution is obtained by solving the jump conditions across shocks plus an ordinary differential equation arising from the self-similarity condition along rarefaction waves, in a similar way as in purely normal flow. The dependence of the solution on the tangential velocities is analysed, and the impact of this result on the development of multi-dimensional relativistic hydrodynamic codes (of Godunov type) is discussed.

1. Introduction

The decay of a discontinuity separating two constant initial states (*Riemann problem*) has played a very important role in the development of numerical hydrodynamic codes in classical (Newtonian) hydrodynamics following the pioneering work of Godunov (1959). Nowadays, most modern high-resolution shock-capturing methods (LeVeque 1992) are based on the exact or approximate solution of Riemann problems between adjacent numerical cells and the development of efficient Riemann solvers has become a research field in numerical analysis in its own right (see e.g. the book by Toro 1997).

Riemann solvers began to be introduced in numerical relativistic hydrodynamics at the beginning of the nineties (Martí, Ibáñez & Miralles 1991). At present, the use of high-resolution shock-capturing methods based on Riemann solvers is considered the best strategy to solve the equations of relativistic hydrodynamics in nuclear physics (heavy ion collisions) and astrophysics (stellar core collapse, supernova explosions, extragalactic jets, gamma-ray bursts). This has caused a rapid development of Riemann solvers for both special and general relativistic hydrodynamics (see e.g. the reviews by Ibáñez & Martí 1999; Martí & Müller 1999).

In a previous paper (Martí & Müller 1994, referred to as Paper I in what follows), we derived the analytical solution of the Riemann problem for an ideal gas in special relativistic hydrodynamics for initial states where the flow is normal to the initial discontinuity. This solution has proven to be a useful for (i) the generation of analytical solutions to test relativistic hydrodynamic codes, and (ii) the development of numerical hydrodynamic codes based on an exact Riemann solver (e.g. Martí & Müller 1996; Wen, Panaitescu & Laguna 1997). Because the solution only holds for

flows which are normal to the initial discontinuity, numerical simulations based on the exact Riemann solver of Paper I are restricted to one-dimensional flows. Balsara (1994) and Dai & Woodward (1997) have circumvented this restriction at the price of constructing multi-dimensional Godunov schemes using a Riemann solver based on the two-shock approximation where the rarefaction wave is treated as a shock wave. An iterative relativistic nonlinear Riemann solver that takes into account the effects of non-vanishing tangential velocity components has already been implemented by Falle & Komissarov (1996) for Riemann problems involving two strong rarefactions. Finally, we note that the effect of the tangential velocity on the properties of simple waves and shocks has usually been ignored in relativistic hydrodynamics, because it is always possible to choose a reference frame in which the tangential velocity vanishes on both sides of the simple wave or shock. In the case of a Riemann problem this reference frame does not exist. The general solution cannot be constructed in terms of the solution of the purely normal flow case and by means of a single Lorentz transformation.

In the following we derive the exact solution of a Riemann problem in Minkowski space–time with arbitrary tangential velocities. The solution can be implemented in multi-dimensional special relativistic hydrodynamic codes based on directional splitting, because it allows the computation of the numerical fluxes at every zone interface. Furthermore, according to recent work by Pons *et al.* (1998), who solve the equations of general relativistic hydrodynamics using special relativistic Riemann solvers, this exact solution can also be implemented in general relativistic hydrodynamic codes. The exact solution also allows one to test the accuracy of other approximate Riemann solvers and codes.

In this paper we closely follow the structure and notation used in Paper I, where one can also find the basic references for the theory of relativistic simple waves and shocks, first discussed by Taub (1948). Two key references in the theory of relativistic fluids are the review by Taub (1978) and the book by Anile (1989). The main idea behind the solution of a Riemann problem (defined by two constant initial states, L and R, to the left and right of their common contact surface) is that the self-similarity of the flow through rarefaction waves and the Rankine–Hugoniot relations across shocks allow one to connect the intermediate states I_* ($I = L, R$) with their corresponding initial states, I. The analytical solution of the Riemann problem in classical hydrodynamics (see e.g. Courant & Friedrichs 1948) rests on the fact that the normal velocity in the intermediate states, $v^n_{I_*}$, can be written as a function of the pressure p_{I_*} in that state (and the flow conditions in state I). Thus, once p_{I_*} is known, $v^n_{I_*}$ and all other unknown state quantities of I_* can be calculated. In order to obtain the pressure p_{I_*} one uses the jump conditions across the contact discontinuity, which are given by

$$p_{L*} = p_{R*}(= p_*), \tag{1.1}$$

$$v^n_{L*}(p_*) = v^n_{R*}(p_*). \tag{1.2}$$

Equation (1.2) is an implicit algebraic equation in p_* and can be solved by means of an iterative method. The function $v^n_{I*}(p_*)$ is constructed by using the relations across the corresponding wave connecting the states I and I_*.

In the case of relativistic hydrodynamics the same procedure can be followed, the major difference with classical hydrodynamics stemming from the role of tangential velocities. While in the classical case the decay of the initial discontinuity does not depend on the tangential velocity (which is constant across shock waves and rarefactions), in relativistic calculations the components of the flow velocity are

coupled through the presence of the Lorentz factor in the equations. In addition, the specific enthalpy also couples with the tangential velocities, which becomes important in the thermodynamically ultrarelativistic regime.

The structure of the paper is the following. First, in § 2 we present the equations of relativistic hydrodynamics for a perfect fluid in three spatial dimensions. In § 3 and § 4 we summarize the properties of the flow across rarefaction waves and shocks, respectively, and explain how to obtain the pressure and velocities behind the corresponding waves as a function of the state ahead the waves. In § 5 we combine the results from the two previous sections to solve the Riemann problem. Finally, in § 6 we discuss the implementation of the solution in numerical relativistic hydrodynamics. Throughout the paper we will recover the corresponding purely normal flow expressions whenever it is of interest.

2. The equations of relativistic hydrodynamics

Let J^μ and $T^{\mu\nu}$ $(\mu, \nu = 0, 1, 2, 3)$ be the components of the density current and the energy-momentum tensor of a perfect fluid, respectively:

$$J^\mu = \rho u^\mu, \tag{2.1}$$

$$T^{\mu\nu} = \rho h u^\mu u^\nu + p\eta^{\mu\nu}, \tag{2.2}$$

where ρ denotes the proper rest-mass density, p the pressure, $h = 1 + \epsilon + p/\rho$ the specific enthalpy, ϵ is the specific internal energy and u^μ is the four-velocity of the fluid, satisfying the normalization condition

$$u^\mu u_\mu = -1 \tag{2.3}$$

(throughout this paper, we will use the summation convention over repeated indices and units in which the speed of light is set to unity). In Cartesian coordinates, $x^\mu = (t, x, y, z)$, the Minkowski metric tensor $\eta^{\mu\nu}$ is given by

$$\eta^{\mu\nu} = \mathrm{diag}(-1, 1, 1, 1). \tag{2.4}$$

The evolution of a relativistic fluid is determined by the conservation equation of rest mass (continuity equation) and energy-momentum

$$J^\mu_{,\mu} = 0, \tag{2.5}$$

$$T^{\mu\nu}_{,\mu} = 0, \tag{2.6}$$

where $_{,\mu}$ stands for the partial derivative with respect to coordinate x^μ. The above system is closed by an equation of state (EOS) which we shall assume as given in the form $p = p(\rho, \epsilon)$.

The normalization condition of the velocity (2.3) leads to

$$u^\mu = W(1, v^x, v^y, v^z), \tag{2.7}$$

where W, the Lorentz factor, is

$$W = (1 - v^2)^{-1/2} \tag{2.8}$$

and

$$v^2 = (v^x)^2 + (v^y)^2 + (v^z)^2. \tag{2.9}$$

The equations of relativistic hydrodynamics admit a conservative formulation which

has been exploited in the last decade to implement high-resolution shock-capturing methods. In Minkowski space–time the equations in this formulation read

$$\boldsymbol{U}_{,t} + \boldsymbol{F}^{(i)}_{,i} = 0, \tag{2.10}$$

where $\boldsymbol{U}$ and $\boldsymbol{F}^{(i)}(\boldsymbol{U})$ $(i = 1, 2, 3)$ are, respectively, the vectors of conserved variables and fluxes:

$$\boldsymbol{U} = (D, S^1, S^2, S^3, \tau)^T, \tag{2.11}$$

$$\boldsymbol{F}^{(i)} = (Dv^i, S^1 v^i + p\delta^{1i}, S^2 v^i + p\delta^{2i}, S^3 v^i + p\delta^{3i}, S^i - Dv^i)^T. \tag{2.12}$$

The conserved variables (the rest-mass density, D, the momentum density, S^i, and the energy density τ) are defined in terms of the *primitive variables*, (ρ, v^i, ϵ), according to

$$D = \rho W, \quad S^i = \rho h W^2 v^i, \quad \tau = \rho h W^2 - p - D. \tag{2.13}$$

System (2.10) is closed by means of an EOS that we shall assume as given in the form

$$p = p(\rho, \varepsilon). \tag{2.14}$$

The sound speed, c_s, is then defined by

$$h c_s^2 = \left.\frac{\partial p}{\partial \rho}\right|_s, \tag{2.15}$$

where s is the specific entropy.

In the case of an ideal gas with constant adiabatic exponent, γ, that we have considered in all the tests shown in this paper, the equation of state is simply

$$p = (\gamma - 1)\rho\varepsilon. \tag{2.16}$$

The hyperbolic character of the equations of relativistic hydrodynamics for causal equations of state and their eigenstructure are well known (e.g. Anile 1989). The complex dependence of the characteristic fields on the tangential velocity in arbitrary (i.e. non-comoving) frames, which is explicitly known (e.g. Donat *et al.* 1998), strongly affects the eigensystem and determines the properties of the waves.

3. Relation between the normal flow velocity and the pressure behind relativistic rarefaction waves

Rarefaction waves are simple waves in which the pressure and the density of a fluid element decreases when crossing them. Choosing the surface of discontinuity to be normal to the x-axis, rarefaction waves would be self-similar solutions of the flow equations depending only the combination $\xi = x/t$. On discarding all the terms with y and z derivatives in equations (2.10) and substituting the derivatives of x and t in terms of the derivatives of ξ, the system reads

$$(v^x - \xi)\frac{\mathrm{d}\rho}{\mathrm{d}\xi} + \{\rho W^2 v^x (v^x - \xi) + \rho\}\frac{\mathrm{d}v^x}{\mathrm{d}\xi} + \rho W^2 v^y (v^x - \xi)\frac{\mathrm{d}v^y}{\mathrm{d}\xi} + \rho W^2 v^z (v^x - \xi)\frac{\mathrm{d}v^z}{\mathrm{d}\xi} = 0, \tag{3.1}$$

$$\rho h W^2 (v^x - \xi)\frac{\mathrm{d}v^x}{\mathrm{d}\xi} + (1 - v^x \xi)\frac{\mathrm{d}p}{\mathrm{d}\xi} = 0, \tag{3.2}$$

$$\rho h W^2 (v^x - \xi)\frac{\mathrm{d}v^y}{\mathrm{d}\xi} - v^y \xi \frac{\mathrm{d}p}{\mathrm{d}\xi} = 0, \tag{3.3}$$

$$\rho h W^2 (v^x - \xi)\frac{\mathrm{d}v^z}{\mathrm{d}\xi} - v^z \xi \frac{\mathrm{d}p}{\mathrm{d}\xi} = 0. \tag{3.4}$$

Equation (3.1) comes from the equation of continuity. The remaining equations come from the momentum conservation. Equations (3.3)–(3.4) reflect the expected result: if the tangential velocities are zero in the chosen state, no tangential flow will develop inside the rarefaction. Finally, instead of considering the conservation of energy, we use the conservation of entropy along fluid lines (following the same reasoning as in Paper I) which provides a relation between $\mathrm{d}p/\mathrm{d}\xi$, $\mathrm{d}\rho/\mathrm{d}\xi$ and $\mathrm{d}h/\mathrm{d}\xi$

$$\frac{\mathrm{d}p}{\mathrm{d}\xi} = hc_s^2\frac{\mathrm{d}\rho}{\mathrm{d}\xi} = \rho\frac{\mathrm{d}h}{\mathrm{d}\xi}. \tag{3.5}$$

Non-trivial similarity solutions exist only if the determinant of system (3.1)–(3.5) vanish. This leads to the condition

$$\xi = \frac{v^x(1-c_s^2) \pm c_s\sqrt{(1-v^2)[1-v^2c_s^2-(v^x)^2(1-c_s^2)]}}{1-v^2c_s^2}, \tag{3.6}$$

the plus and minus sign corresponding to rarefaction waves propagating to the left $\mathscr{R}_{\leftarrow}$ and right $\mathscr{R}_{\rightarrow}$, respectively. It is important to note that the two solutions for ξ correspond to the maximum and minimum eigenvalues of the Jacobian matrix associated with the fluxes $\boldsymbol{F}^{(x)}(\boldsymbol{U})$ (see e.g. Donat *et al.* 1998), generalizing the result found for a vanishing tangential velocity in Paper I (equation (32)).

After some manipulation, the system (3.1)–(3.5) can be reduced to just one ordinary differential equation (ODE) and two algebraic conditions:

$$\rho hW^2(v^x-\xi)\mathrm{d}v^x + (1-\xi v^x)\mathrm{d}p = 0, \tag{3.7}$$

$$hWv^y = \text{constant}, \tag{3.8}$$

$$hWv^z = \text{constant}, \tag{3.9}$$

with ξ constrained by (3.6). From equations (3.8) and (3.9) it follows that v^y/v^z = constant, i.e. the tangential velocity does not change direction along rarefaction waves and it is only allowed to change its absolute value. Notice that, in a kinematical sense, the Newtonian limit ($v^i \ll 1$) leads to $W = 1$, but equations (3.8) and (3.9) do not reduce to the classical limit $v^{y,z}$ = constant, because the specific enthalpy still couples the tangential velocities. Thus, even for slow or moderately relativistic flows ($W \approx 1$), the Riemann solution presented in this paper must be employed for thermodynamically relativistic situations ($h > 1$). The same result can be deduced from the Rankine–Hugoniot relations for shock waves (see the next section).

Using (3.6), the ODE (3.7) can be rewritten as

$$\frac{\mathrm{d}v^x}{\mathrm{d}p} = \pm\frac{1}{\rho hW^2c_s}\frac{1}{\sqrt{1+g(\xi_\pm, v^x, v^t)}}, \tag{3.10}$$

where $v^t = \sqrt{(v^y)^2+(v^z)^2}$ is the absolute value of the tangential velocity and

$$g(\xi_\pm, v^x, v^t) = \frac{(v^t)^2(\xi_\pm^2-1)}{(1-\xi_\pm v^x)^2}. \tag{3.11}$$

The sign of $\xi_\pm$ corresponds to the sign chosen in (3.6). In the limit of zero tangential velocities, $v^t = 0$, the constants in (3.8), (3.9) are zero and the function g does not

contribute. In this limit and in case of an ideal-gas EOS one has

$$W^2 \mathrm{d}v^x = \pm \frac{c_s}{\gamma p}\mathrm{d}p = \pm \frac{c_s}{\rho}\mathrm{d}\rho, \tag{3.12}$$

recovering expression (30) in Paper I.

Considering that in a Riemann problem the state ahead of the rarefaction wave is known, the integration of (3.10) allows one to connect the states ahead (a) and behind (b) the rarefaction wave. Moreover, using (3.6), the EOS, and the following relation obtained from the constraint $hWv^t = \text{constant}$:

$$v_b^t = h_a W_a v_a^t \left\{ \frac{1-(v_b^x)^2}{h_b^2 + (h_a W_a v_a^t)^2} \right\}^{1/2}, \tag{3.13}$$

the ODE can be integrated, the solution being a function of p_b only. This can be stated in compact form as

$$v_b^x = \mathscr{R}^a_{\rightleftharpoons}(p_b). \tag{3.14}$$

Function $\mathscr{R}^a_{\rightleftharpoons}(p)$ is shown in figure 1, for different values of the tangential velocity v^t in state a, the various branches of the curves corresponding to rarefaction waves propagating towards or away from a. Rarefaction waves move towards (away from) a, if the pressure inside the rarefaction is smaller (larger) than p_a. In a Riemann problem the state a is ahead of the wave and only those branches corresponding to waves propagating towards a in figure 1 must be considered. Moreover, one can discriminate between waves propagating towards the left and right by taking into account that the initial left (right) state can only be reached by a wave propagating towards the left (right). The presence of a tangential velocity in the limiting state restricts the value of the normal velocity within the rarefaction wave to smaller values as is clearly seen from figure 1. Once the pressure in the post-wave state has been obtained, the corresponding tangential velocity follows from (3.13) (see figure 1b).

4. Relation between post-shock flow velocities and pressure for relativistic shock waves

The Rankine–Hugoniot conditions relate the states on both sides of a shock and are based on the continuity of the mass flux and the energy-momentum flux across shocks. Their relativistic version was first obtained by Taub (1948) (see also Taub 1978 and Königl 1980).

If Σ is a hyper-surface in Minkowski space–time across which ρ, u^μ and $T^{\mu\nu}$ are discontinuous, the relativistic Rankine–Hugoniot conditions are given by

$$[\rho u^\mu] n_\mu = 0, \tag{4.1}$$

$$[T^{\mu\nu}] n_\nu = 0, \tag{4.2}$$

where n_μ is the unit normal to Σ, and where we have used the notation

$$[F] = F_a - F_b, \tag{4.3}$$

F_a and F_b being the boundary values of F on the two sides of Σ.

Considering Σ as normal to the x-axis, the unitarity of n_ν allows one to write it as

$$n^\nu = W_s(V_s, 1, 0, 0), \tag{4.4}$$

where V_s is interpreted as the coordinate velocity of the hyper-surface that defines

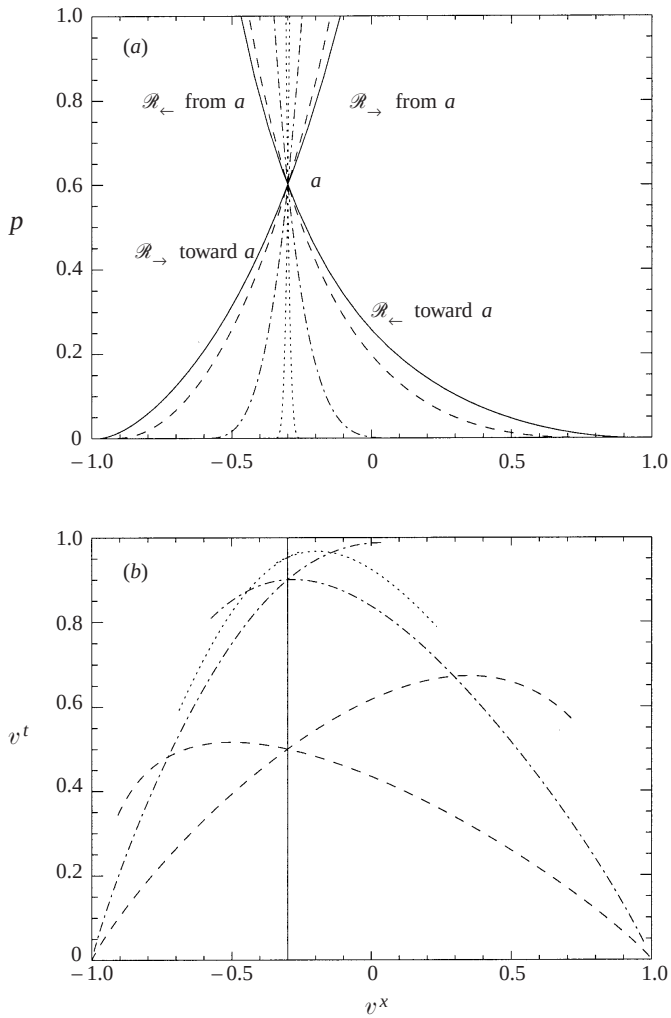

FIGURE 1. Loci of states which can be connected with a given state a by means of relativistic rarefaction waves propagating to the left ($\mathscr{R}_\leftarrow$) and to the right ($\mathscr{R}_\rightarrow$) and moving towards or away from a. (a) Pressure versus v^x; (b) tangential velocity versus v^x. Solutions for different values of the tangential velocity $v^t = 0, 0.5, 0.9, 0.953$ correspond to solid, dashed, dashed-dotted and dotted lines, respectively. The state a is characterized by $p_a = 0.6$, $\rho_a = 1.0$, and $v_a^x = -0.3$. An ideal-gas EOS with $\gamma = 5/3$ was assumed.

the position of the shock wave and W_s is the Lorentz factor of the shock,

$$W_s = \frac{1}{\sqrt{1 - V_s^2}}. \tag{4.5}$$

Equation (4.1) allows one to introduce the invariant mass flux across the shock:

$$j \equiv W_s D_a (V_s - v_a^x) = W_s D_b (V_s - v_b^x). \tag{4.6}$$

According to our definition, j is positive for shocks propagating to the right. Note that our convention differs from that of both Landau & Lifshitz (1987) and Courant & Friedrichs (1948), but is the same as in Paper I.

Next, the Rankine–Hugoniot conditions (4.1), (4.2) can be written in terms of the

conserved quantities D, S^j and τ, and of the mass flux as follows:

$$[v^x] = -\frac{j}{W_s}\left[\frac{1}{D}\right], \tag{4.7}$$

$$[p] = \frac{j}{W_s}\left[\frac{S^x}{D}\right], \tag{4.8}$$

$$\left[\frac{S^y}{D}\right] = 0, \tag{4.9}$$

$$\left[\frac{S^z}{D}\right] = 0, \tag{4.10}$$

$$[v^x p] = \frac{j}{W_s}\left[\frac{\tau}{D}\right]. \tag{4.11}$$

We note that in deriving equations (4.7)–(4.11) we have made use of the fact that the mass flux is non-zero across a shock. The conditions across a tangential discontinuity imply continuous pressure and normal velocity (by setting $j = 0$ in equations (4.7), (4.8) and (4.11)), and an arbitrary jump in the tangential velocity.

Equations (4.9) and (4.10) imply that the quantity $hWv^{y,z}$ is constant across a shock wave and, hence, that the orientation of the tangential velocity does not change. The latter result also holds for rarefaction waves (see §3). Equations (4.7), (4.8) and (4.11) are formally identical to the corresponding equations in Paper I (equations (47)–(49)) and can be manipulated in the same way to obtain v_b^x as a function of p_b, j and V_s. Using the relation $S^x = (\tau + p + D)v^x$, and after some algebra, one finds

$$v_b^x = \left(h_a W_a v_a^x + \frac{W_s(p_b - p_a)}{j}\right)\left(h_a W_a + (p_b - p_a)\left(\frac{W_s v_a^x}{j} + \frac{1}{\rho_a W_a}\right)\right)^{-1}. \tag{4.12}$$

This expression looks like that obtained for vanishing tangential velocity, but its presence is hidden within the Lorentz factor in state a, W_a. From (4.9) and (4.10) expressions for v_b^y and v_b^z can be derived:

$$v_b^{y,z} = h_a W_a v_a^{y,z}\left[\frac{1 - (v_b^x)^2}{h_b^2 + (h_a W_a v_a^{y,z})^2}\right]^{1/2}. \tag{4.13}$$

The final step is to express j and V_s as a function of the post-shock pressure. From the definition of the mass flux we obtain

$$V_s^{\pm} = \frac{\rho_a^2 W_a^2 v_a^x \pm |j|\sqrt{j^2 + \rho_a^2 W_a^2 (1 - v_a^{x2})}}{\rho_a^2 W_a^2 + j^2}, \tag{4.14}$$

where V_s^+ (V_s^-) corresponds to shocks propagating to the right (left).

The Taub adiabat (Thorne 1973), which relates (only) thermodynamic quantities on both sides of the shock, and the EOS can be used to derive the desired expressions. The Taub adiabat, the relativistic version of the Hugoniot adiabat, is obtained by multiplying (4.2) first by $(hu_\mu)_a$ and subsequently by $(hu_\mu)_b$, and by summing the resulting expressions. After some algebra one finds

$$[h^2] = \left(\frac{h_b}{\rho_b} + \frac{h_a}{\rho_a}\right)[p]. \tag{4.15}$$

In the general case, the above nonlinear equation must be solved together with the

EOS to obtain the post-shock enthalpy as a function of p_b. In the case of the ideal-gas EOS with constant adiabatic index, the post-shock density ρ_b can be easily eliminated and the Taub adiabat can be rewritten in the form (see Paper I)

$$h_b^2\left(1+\frac{(\gamma-1)(p_a-p_b)}{\gamma p_b}\right)-\frac{(\gamma-1)(p_a-p_b)}{\gamma p_b}h_b+\frac{h_a(p_a-p_b)}{\rho_a}-h_a^2=0\,, \tag{4.16}$$

which is a quadratic equation for the post-shock enthalpy h_b as a function of p_b. One of the two roots is always negative and must be discarded as a physical solution.

Next multiplying (4.2) by n_μ and using the definition of the relativistic mass flux (4.6) one obtains

$$j^2=\frac{-[p]}{[h/\rho]}, \tag{4.17}$$

which after using the EOS to eliminate ρ_b and inserting the physical solution of (4.15) gives the square of the mass flux j^2 as a function of p_b.

Using the positive (negative) root of j^2 for shock waves propagating towards the right (left), equation (4.17) allows one to obtain the desired relation between the post-shock normal velocity v_b^x and the post-shock pressure p_b. In a compact way the relation reads

$$v_b^x=\mathscr{S}^a_{\rightleftharpoons}(p_b). \tag{4.18}$$

The function $\mathscr{S}^a_{\rightleftharpoons}(p)$ is shown in figure 2 for several values of the tangential velocity v^t in state a. Its various branches correspond to shock waves propagating towards or away from a. In order to select the relevant branch of the function $\mathscr{S}^a_{\rightleftharpoons}(p)$ (figure 2) the same argumentation as in the case of rarefaction waves can be used (see § 3). When v_b^x is known, (4.13) can be used to determine v^y and v^z in the post-shock state.

5. The solution of the Riemann problem with arbitrary tangential velocities

The decay of an initial discontinuity gives rise, in general, to three elementary nonlinear waves (see e.g. Landau & Lifshitz 1987). Two of them can be shocks or rarefaction waves, one moving towards the initial left-hand state and the other towards the initial right-hand state. Between them, two new states appear, namely L_* and R_*, separated from each other by the third wave, which is a contact discontinuity moving along with the fluid. Across the contact discontinuity pressure and normal velocity are constant, while the density and the tangential velocity exhibit a jump. Accordingly, the time evolution of a Riemann problem can be represented as

$$I\ \rightarrow\ L\ \mathscr{W}_{\leftarrow}\ L_*\ \mathscr{C}\ R_*\ \mathscr{W}_{\rightarrow}\ R, \tag{5.1}$$

where $\mathscr{W}$ and $\mathscr{C}$ denote a simple wave (shock or rarefaction) and a contact discontinuity, respectively. The arrows ($\leftarrow/\rightarrow$) indicate the direction (left/right) from which fluid elements enter the corresponding wave.

As in the Newtonian case, the compressive character of shock waves (density and pressure rise across the shock) allows us to discriminate between shocks ($\mathscr{S}$) and rarefaction waves ($\mathscr{R}$):

$$\mathscr{W}_{\leftarrow(\rightarrow)}=\begin{cases}\mathscr{R}_{\leftarrow(\rightarrow)}, & p_b\leqslant p_a\\ \mathscr{S}_{\leftarrow(\rightarrow)}, & p_b>p_a,\end{cases} \tag{5.2}$$

where p is the pressure and subscripts a and b denote quantities ahead of and behind the wave. For the Riemann problem $a\equiv L(R)$ and $b\equiv L_*(R_*)$ for $\mathscr{W}_{\leftarrow}$ and $\mathscr{W}_{\rightarrow}$,

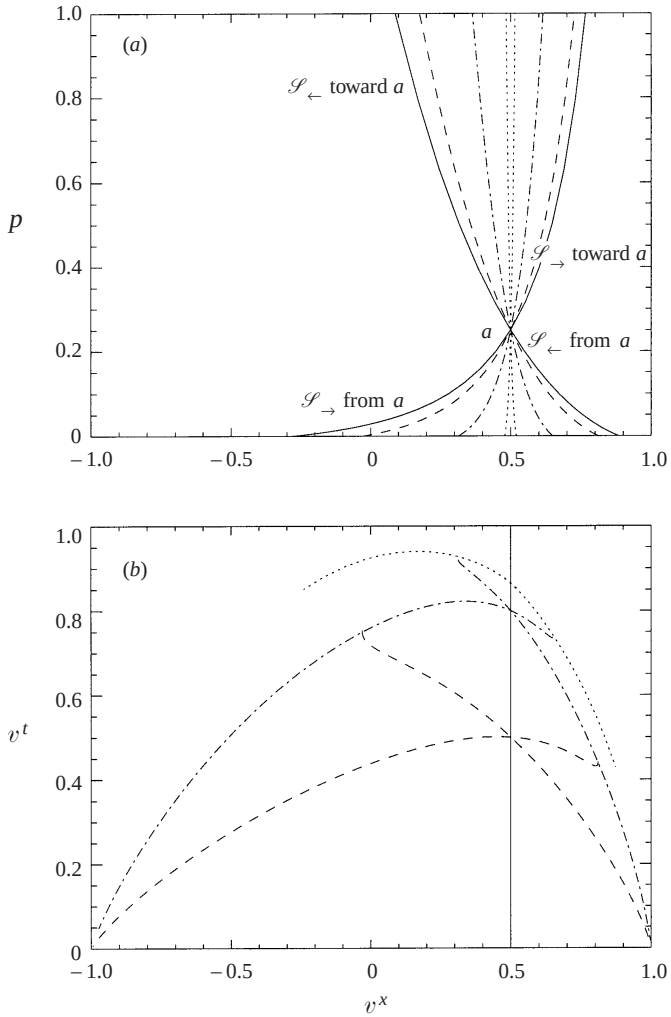

FIGURE 2. Loci of states which can be connected with a given state a by means of relativistic shock waves propagating to the left ($\mathscr{S}_\leftarrow$) and to the right ($\mathscr{S}_\rightarrow$) and moving towards or away from a. (a) Pressure versus v^x; (b) tangential velocity versus v^x. Solutions for different values of the tangential velocity $v^t = 0, 0.5, 0.8, 0.865$ correspond to solid, dashed, dashed-dotted and dotted lines, respectively. The state a is characterized by $p_a = 0.25$, $\rho_a = 1.0$, and $v^x_a = -0.5$. An ideal-gas EOS with $\gamma = 5/3$ was assumed.

respectively. Thus, the possible types of decay of an initial discontinuity can be reduced to

$$(a)\ I \rightarrow L\ \mathscr{S}_\leftarrow\ L_*\ \mathscr{C}\ R_*\ \mathscr{S}_\rightarrow\ R \quad p_L < p_{L*} = p_{R*} > p_R, \tag{5.3}$$

$$(b)\ I \rightarrow L\ \mathscr{S}_\leftarrow\ L_*\ \mathscr{C}\ R_*\ \mathscr{R}_\rightarrow\ R \quad p_L < p_{L*} = p_{R*} \leqslant p_R, \tag{5.4}$$

$$(c)\ I \rightarrow L\ \mathscr{R}_\leftarrow\ L_*\ \mathscr{C}\ R_*\ \mathscr{R}_\rightarrow\ R \quad p_L \geqslant p_{L*} = p_{R*} \leqslant p_R. \tag{5.5}$$

The solution of the Riemann problem consists in finding the intermediate states, L_* and R_*, as well as the positions of the waves separating the four states (which only depend on L, L_*, R_* and R). The functions $\mathscr{W}_\rightarrow$ and $\mathscr{W}_\leftarrow$ allow one to determine the functions $v^x_{R*}(p)$ and $v^x_{L*}(p)$, respectively. The pressure p_* and the flow velocity v^x_* in

v_L^t	v_R^t	ρ_{L*}	ρ_{R*}	p_*	v_*^x	V_s	ξ_h	ξ_t
0	0	0.0916	10.4	18.6	0.960	0.987	−0.816	+0.668
0	0.90	0.151	14.6	42.8	0.913	0.973	−0.816	+0.379
0	0.99	0.289	43.6	127.0	0.767	0.927	−0.816	−0.132
0.90	0	0.00583	3.44	0.189	0.328	0.452	−0.525	+0.308
0.90	0.90	0.0149	4.46	0.904	0.319	0.445	−0.525	+0.282
0.90	0.99	0.0572	7.83	8.48	0.292	0.484	−0.525	+0.197
0.99	0	0.00199	1.91	0.0316	0.099	0.208	−0.196	+0.096
0.99	0.90	0.0038	2.90	0.0927	0.098	0.153	−0.196	+0.094
0.99	0.99	0.0129	4.29	0.706	0.095	0.140	−0.196	+0.085

TABLE 1. Solution of the relativistic Riemann problem at $t = 0.4$ with initial data $p_L = 10^3$, $\rho_L = 1.0$, $v_L^x = 0$, $p_R = 10^{-2}$, $\rho_R = 1.0$ and $v_R^x = 0$ for nine different combinations of tangential velocities in the left (v_L^t) and right (v_R^t) initial state. An ideal-gas EOS with $\gamma = 5/3$ was assumed. The various quantities in the table are: the density in the intermediate state to the left (ρ_{L*}) and right (ρ_{R*}) of the contact discontinuity, the pressure in the intermediate state (p_*), the flow speed in the intermediate state (v_*^x), the speed of the shock wave (V_s), and the velocities of the head (ξ_h) and tail (ξ_t) of the rarefaction wave.

the intermediate states are then given by the condition

$$v_{R*}^x(p) = v_{L*}^x(p) = v_*^x. \tag{5.6}$$

When p_* and v_*^x have been obtained the remaining quantities can be computed. The EOS gives the specific internal energy and the remaining state variables of the intermediate state I_* can be calculated using the relations between I_* and the respective initial state I given through the corresponding wave. In particular, the tangential velocities can be calculated from (3.8)–(3.9) for rarefaction waves and from the Rankine–Hugoniot jump conditions (4.9)–(4.10) for shock waves. Notice that the solution of the Riemann problem depends on the modulus of v^t, but not on the direction of the tangential velocity. Figure 3 shows the solution of a particular Riemann problem (Sod 1978) for different values of the tangential velocity $v^y = 0, 0.5, 0.9, 0.99$. The crossing point of any two lines in figure 3(*a*) gives the pressure and the normal velocity in the intermediate states. The range of possible solutions in the (p, v^x)-plane is marked by the shaded region. Whereas the pressure in the intermediate state can take any value between p_L and p_R, the normal flow velocity can be arbitrarily close to zero in the case of an extremely relativistic tangential flow. The values of the tangential velocity in the states L_* and R_* are obtained from the value of the corresponding functions at v^x in figure 3(*b*).

To study the influence of tangential velocities on the solution to a Riemann problem, we have calculated the solution of a standard test involving the propagation of a relativistic blast wave produced by a large jump in the initial pressure distribution (see Martí & Müller 1999) for different combinations of v_L^t and v_R^t. The initial data are $p_L = 10^3$, $\rho_L = 1$, $v_L^x = 0$; $p_R = 10^{-2}$, $\rho_R = 1$, $v_R^x = 0$ and the nine possible combinations of $v_{L,R}^t = 0, 0.9, 0.99$. The results are given in figure 4 and table 1.

The speeds of the waves propagating to the left and right, respectively, tend to zero in the limit of $v_{L,R}^t \to 1$. This result is easily deduced from (3.6) which gives the velocities of the head (ξ_h) and tail (ξ_t) of the rarefaction wave, and from (4.14) which gives the shock speed (V_s). These three velocities tend to the normal velocity

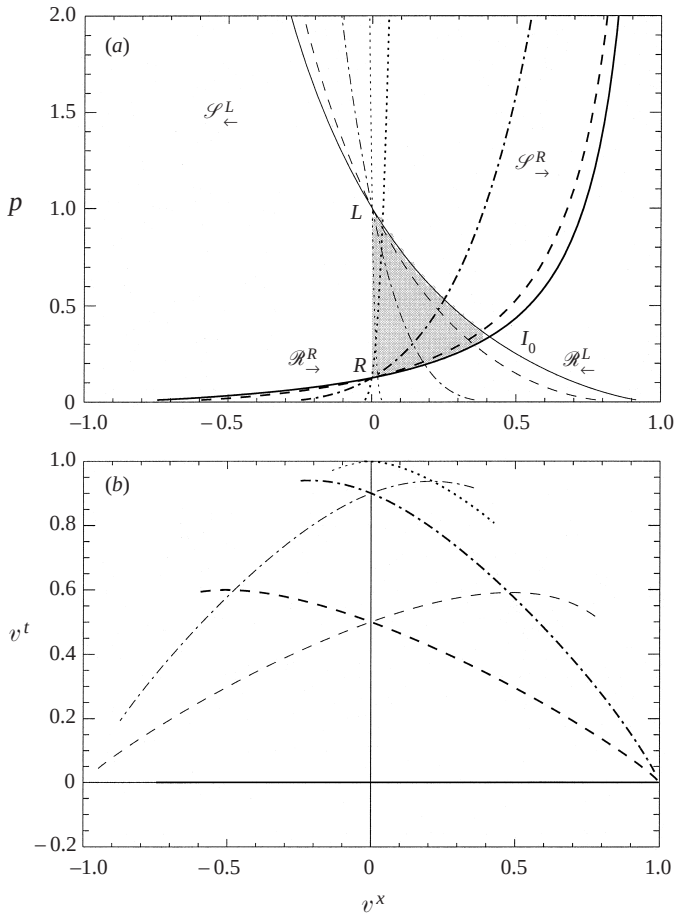

FIGURE 3. Graphical solution in the (p, v^x)-plane (a) and in the (v^t, v^x)-plane (b) of the relativistic Riemann problem with initial data $p_L = 1.0$, $\rho_L = 1.0$, $v^x_L = 0$; $p_R = 0.1$, $\rho_R = 0.125$ and $v^x_R = 0$ for different values of the tangential velocity $v^t = 0, 0.5, 0.9, 0.999$, represented by solid, dashed, dashed-dotted and dotted lines, respectively. An ideal-gas EOS with $\gamma = 1.4$ was assumed. The crossing point of any two lines in (a) gives the pressure and the normal velocity in the intermediate states. The value of the tangential velocity in the states L_* and R_* is obtained from the value of the corresponding functions at v^x in (b), and I_0 gives the solution for vanishing tangential velocity. The range of possible solutions is given by the shaded region in (a).

ahead of the wave (v^x_a) when the corresponding tangential velocity (v^t_a) tends to $v^t_{max} = \sqrt{1 - (v^x_a)^2}$.

Although the structure of the solution remains the same (left-propagating rarefaction wave, right-propagating blast wave) the values in the constant intermediate states change by a large amount. The results show (see figure 4 and table 1) that ξ_h remains constant as long as v^t_L is constant. The value of ξ_h only depends on the left-hand state, and decreases with increasing v^t_L. The pressure in the intermediate state, p_*, increases with increasing v^t_R due to the larger effective inertia of the right-hand state (because of the increase of the Lorentz factor of the right-hand state). The velocity of the shock is determined by the competing effects of an increased p_* and the larger inertia of the right state. The shape of the function $\mathscr{R}^a_{\rightleftharpoons}(p)$ (see figure 1) and its dependence on v^t_L shows that both p_* and v^x_* decrease with increasing v^t_L. On the other hand, as

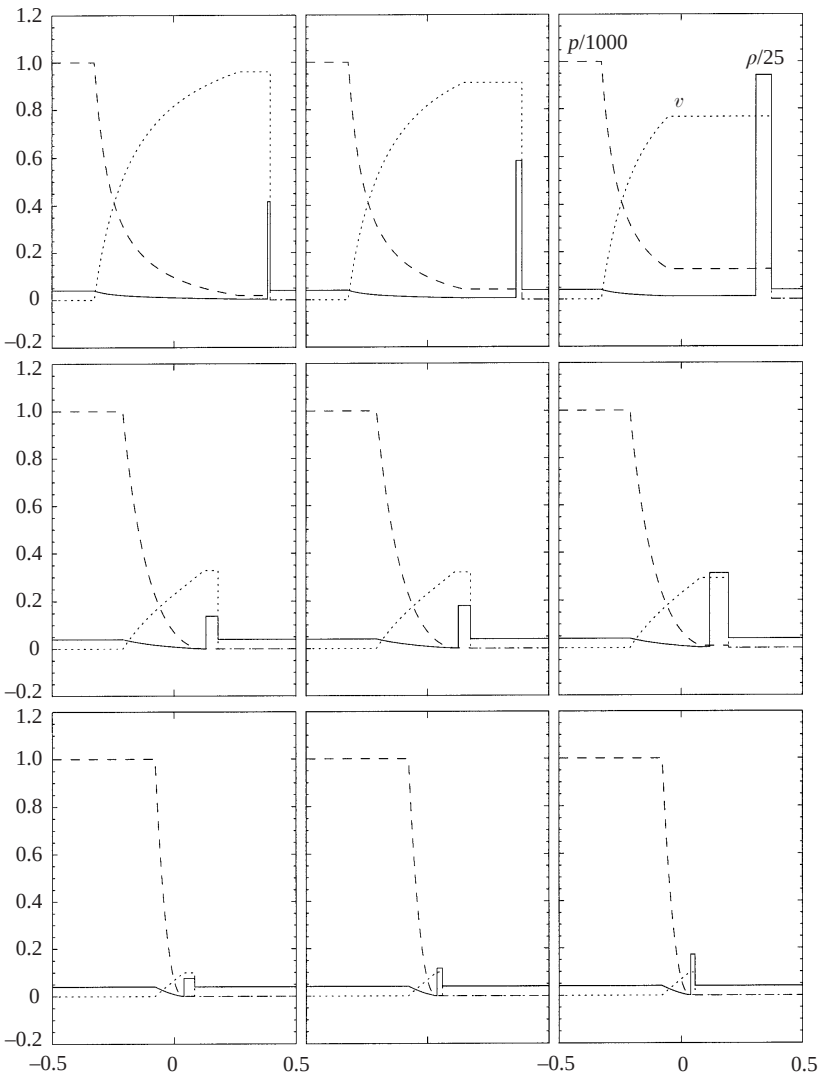

FIGURE 4. Analytical pressure (dashed), density (solid) and flow velocity (dotted) profiles at $t = 0.4$ for the relativistic Riemann problem with initial data $p_L = 10^3$, $\rho_L = 1.0$, $v_L^x = 0$; $p_R = 10^{-2}$, $\rho_R = 1.0$ and $v_R^x = 0$, varying the values of the tangential velocities. From left to right, $v_R^t = 0, 0.9, 0.99$ and from top to bottom $v_L^t = 0, 0.9, 0.99$. An ideal-gas EOS with $\gamma = 5/3$ was assumed.

a change in v_L^t does not alter the thermodynamic state, the flow evolution across the rarefaction wave is along the same adiabat for any value of v_L^t. This explains why ρ_{L*} gets smaller with increasing v_L^t (consistently with the decrease of pressure). Thus, the net effect of tangential velocities on rarefaction waves is to evolve further along the adiabat, and to reach smaller intermediate pressure values.

6. Conclusions

We have obtained the exact solution of the Riemann problem in special relativistic hydrodynamics with arbitrary tangential velocities. Unlike in Newtonian hydrodynamics, tangential velocities are coupled with the rest of variables through the Lorentz

factor, present in all terms in all equations. It strongly affects the solution, especially for ultra-relativistic tangential flows. The specific enthalpy acts as a coupling factor, too. It modifies the solution in thermodynamically relativistic situations (energy density and pressure comparable to or larger than the proper rest-mass density) even in slow flows.

Our solution has interesting practical applications. First, it can be used to check the different approximate relativistic Riemann solvers developed by various authors in the past decade, and to test multi-dimensional hydrodynamic codes based on directional splitting. Second, it can be used to construct multi-dimensional relativistic Godunov-type methods. The latter project is currently in progress and will be reported elsewhere. Finally, using the procedure described by Pons *et al.* (1998) the exact solution can be used as a building block in a general relativistic hydrodynamic code.

The computational cost of the exact Riemann solver derived above is comparable to the one presented by Martí & Müller (1994) which is valid for purely normal flows. Hence, when our exact Riemann solver is applied to multi-dimensional flow problems, the difference in efficiency with respect to most linearized Riemann solvers is reduced.

This work has been supported by the Spanish DGICYT grant PB97-1432, and by the agreement between the Spanish CSIC and the Max-Planck-Gesellschaft. J. A. P. acknowledges financial support from the Spanish Ministerio de Educación y Ciencia (FPI grant). We acknowledge referee B for his interesting comments which helped us to improve the quality of the manuscript.

REFERENCES

Anile, A. M. 1989 *Relativistic Fluids and Magnetofluids*. Cambridge University Press.

Balsara, D. S. 1994 Riemann solver for relativistic hydrodynamics. *J. Comput. Phys.* **114**, 284.

Courant, R. & Friedrichs, K. O. 1948 *Supersonic Flows and Shock Waves*. Interscience.

Dai, W. & Woodward, P. R. 1997 An iterative Riemann solver for relativistic hydrodynamics. *SIAM J. Sci. Comput.* **18**, 982.

Donat, R., Font, J. A., Ibañez, J. M. & Marquina, A. 1998 A flux-split algorithm applied to relativistic flows. *J. Comput. Phys.*, **146**, 58.

Falle, S. A. E. G. & Komissarov, S. S. 1996 An upwind numerical scheme for relativistic hydrodynamics with a general equation of state. *Mon. Not. R. Astron. Soc.* **278**, 586.

Godunov, S. K. 1959 A finite difference method for the numerical computation and discontinuous solutions of the equations of fluid dynamics. *Mat. Sb.* **47**, 271.

Ibañez, J. M. & Martí, J. M. 1999 Riemann solvers in relativistic astrophysics. *J. Comput. Appl. Maths* **109**, 173–211.

Königl, A. 1980 Relativistic gas dynamics in two dimensions. *Phys. Fluids* **23**, 1083.

Landau, L. D. & Lifshitz, E. M. 1987 *Fluid Mechanics, 2nd Edn.*, Pergamon.

LeVeque, R. J. 1992 *Numerical Methods for Conservation Laws, 2nd edn.*, Birkhäuser.

Martí, J. M., Ibañez, J. M. & Miralles, J. A. 1991 Numerical relativistic hydrodynamics: local characteristic approach. *Phys. Rev.* D **43**, 3794.

Martí, J. M. & Müller, E. 1994 The analytical solution of the Riemann problem in relativistic hydrodynamics. *J. Fluid Mech.* **258**, 317 (referred to herein as Paper I).

Martí, J. M. & Müller, E. 1996 Extension of the piecewise parabolic method to one-dimensional relativistic hydrodynamics. *J. Comput. Phys.* **123**, 1.

Martí, J. M. & Müller, E. 1999 Numerical hydrodynamics in special relativity. *Living Reviews in General Relativity* (http://www.livingreviews.org). Pub. No. 1999-3, in press; also astro-ph/9906333.

Pons, J. A., Font, J. A., Martí, J. M., Ibañez, J. M. & Miralles, J. A. 1998 General relativistic hydrodynamics with special relativistic Riemann solvers. *Astron. Astrophys.* **339**, 638.

Sod, G. A. 1978 A survey of several finite difference methods for systems of nonlinear hyperbolic conservation laws. *J. Comput. Phys.* **27**, 1.

Taub, A. H. 1948 Relativistic Rankine–Hugoniot relations. *Phys. Rev.* **74**, 328.

Taub, A. H. 1978 Relativistic fluid mechanics. *Ann. Rev. Fluid Mech.* **10**, 32.

Thorne, K. S. 1973 Relativistic shocks: the Taub adiabat. *Astrophys. J.* **179**, 897.

Toro, E. 1997 *Riemann Solvers and Numerical Methods for Fluid Dynamics.* Springer.

Wen, L., Panaitescu, A. & Laguna, P. 1997 A shock-patching code for ultra-relativistic fluid flow. *Astrophys. J.* **486**, 919.